

## Supporting Information

### Ion Storage Performance of A polymer for mono-, di- and tri-valent Metal Ions in Non-aqueous Electrolytes

Debashis Tripathy, H. M. Vishwanatha, M. N. K. Harish and Srinivasan Sampath\*

Email: [sampath@iisc.ac.in](mailto:sampath@iisc.ac.in)

## **Experimental**

### **Materials used**

Dioxolane (DOL), 1,2-dimethoxyethane (DME), benzoquinone, acetonitrile (AN), pyrrole, 1-butyl-3-methyl imidazolium chloride (BMImCl), Li and Al foils were purchased from Sigma, USA. Aluminium chloride (AlCl<sub>3</sub>) and zinc foil were obtained from Alfa Aesar, USA. Lithium bis(trifluoromethanesulfonyl)imide (LiTFSI) and zinc bis(trifluoromethanesulfonyl)imide (ZnTFSI) were purchased from Solvionic, France.

### **Synthesis of 2DQP**

The polymer was synthesized by following the method reported by Yano et al. (ref. 27 in the main manuscript). Briefly, pyrrole (30 mmol) and benzoquinone (30 mmol) were taken in separate glass vials and kept inside a closed glass vessel of 250 ml volume. The vessel was then transferred to an oven maintained at 60 °C and kept there for 48 h at atmospheric pressure. The polymer was obtained as black powder. Further, it was purified by washing with acetone several times followed by vacuum drying.

### **Electrolyte preparation**

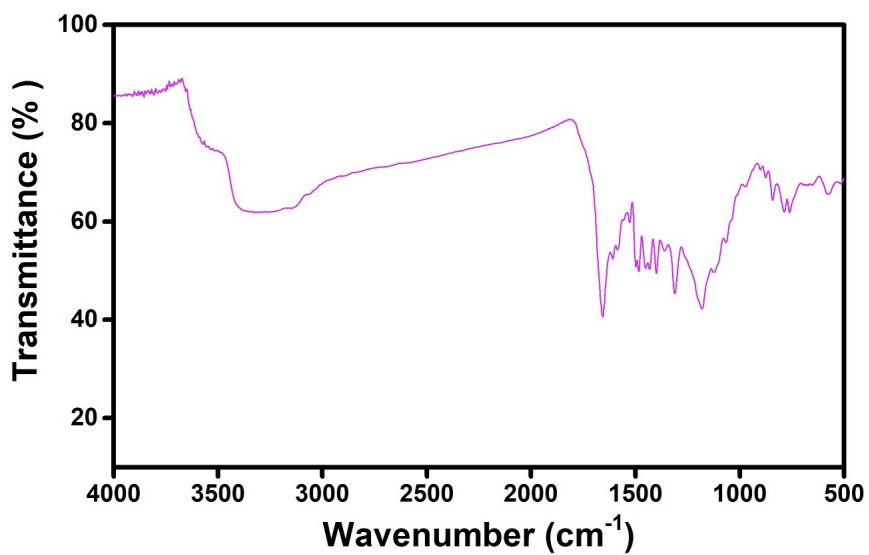
The electrolyte for LIBs was prepared by taking DOL and DME in 1:1 v/v to which an appropriate amount of LiTFSI was added to get 2 M LiTFSI in DOL-DME as electrolyte. Similarly, the electrolyte for ZIBs was prepared by dissolving required amount of ZnTFSI in acetonitrile to obtain 0.5 M concentration. BMImCl-AlCl<sub>3</sub> (1:1.5) was used as electrolyte for AIBs. AlCl<sub>3</sub> was added slowly to BMImCl in a molar ratio of 1.5:1, and then the mixture was stirred for overnight.

### **Characterization**

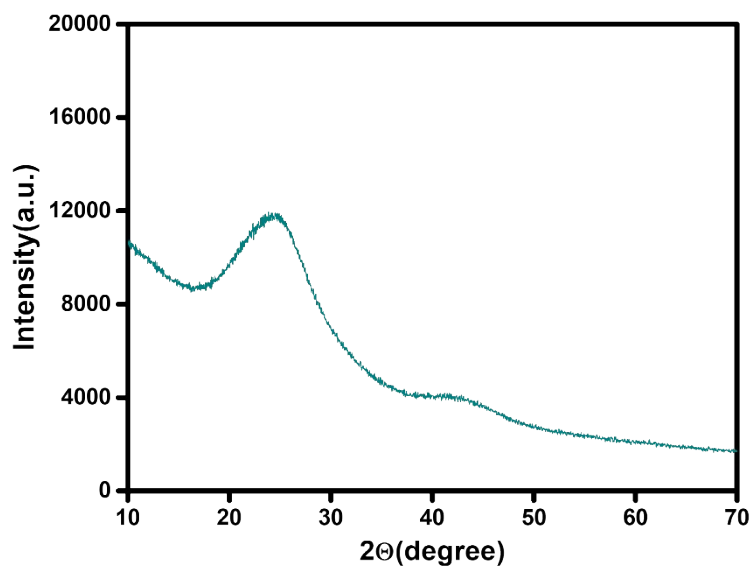
The synthesized polymer was characterized by Fourier transform infrared (FTIR), powder X-ray diffraction (XRD) and X-ray photoelectron spectroscopy (XPS) techniques, scanning electron microscopy (SEM) and transmission electron microscopy (TEM). The FTIR spectra were recorded using Perkin Elmer FTIR spectrometer. XRD measurements were carried out using Philips analytical (PAN Analytical) X-ray BV diffractometer (The Netherlands) with Cu K $\alpha$  ( $\lambda = 1.5418 \text{ \AA}$ ) as the X-ray source. Morphology of the samples were obtained using field emission scanning electron microscopy (FESEM, Carl Zeiss ultra 55) and transmission electron microscope (TEM, Jeol). XPS data were obtained using Thermo Fischer Scientific K-alpha instrument with Al K $\alpha$  as X-ray source.

## **Electrochemical measurements**

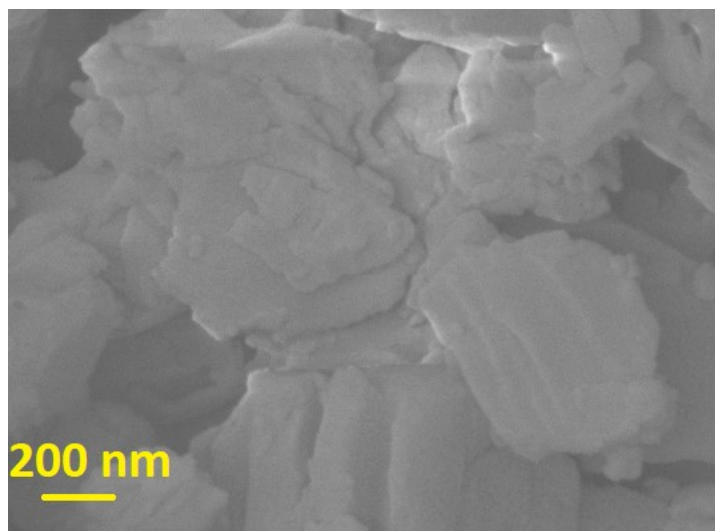
All the electrochemical measurements were carried out using coin-type cells (CR2032). The cells were assembled, and the electrolytes were prepared inside an Argon filled glove box (Jacomex) with moisture and oxygen level below 1 ppm. Li, Zn and Al foils were used as negative electrodes and glass microfiber (Whatman) as separator, respectively. The positive electrodes were prepared by coating the slurry made of 2DQP, acetylene black and polyvinylidene fluoride (PVDF) in 4:5:1 ratio respectively with few drops of N-methyl pyrrolidine (NMP) on carbon paper and then vacuum dried at 80 C for 12 h. For AIBs, the electrodes were prepared by coating the slurry on Mo foil. Cyclic voltammetry (CV) experiments were carried out using Biologic instrument and galvanostatic charge-discharge experiments were carried out in Arbin (USA) and Biologic (France) instruments.



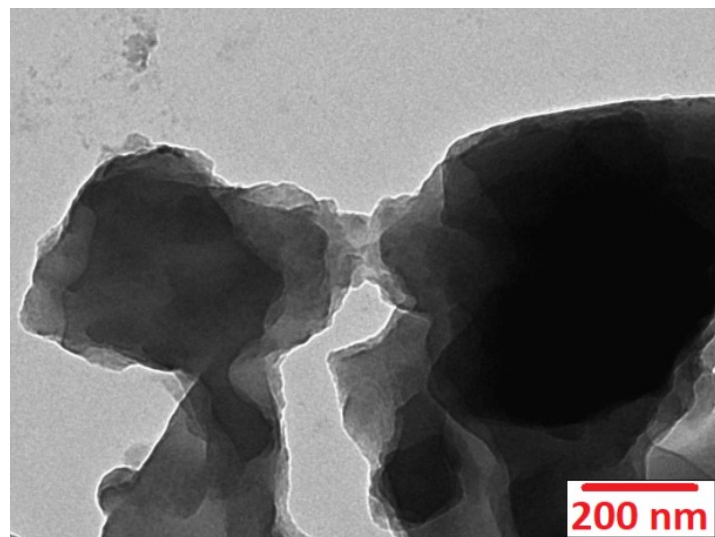
**Fig. S1.** Infrared spectrum of the as prepared polymer.



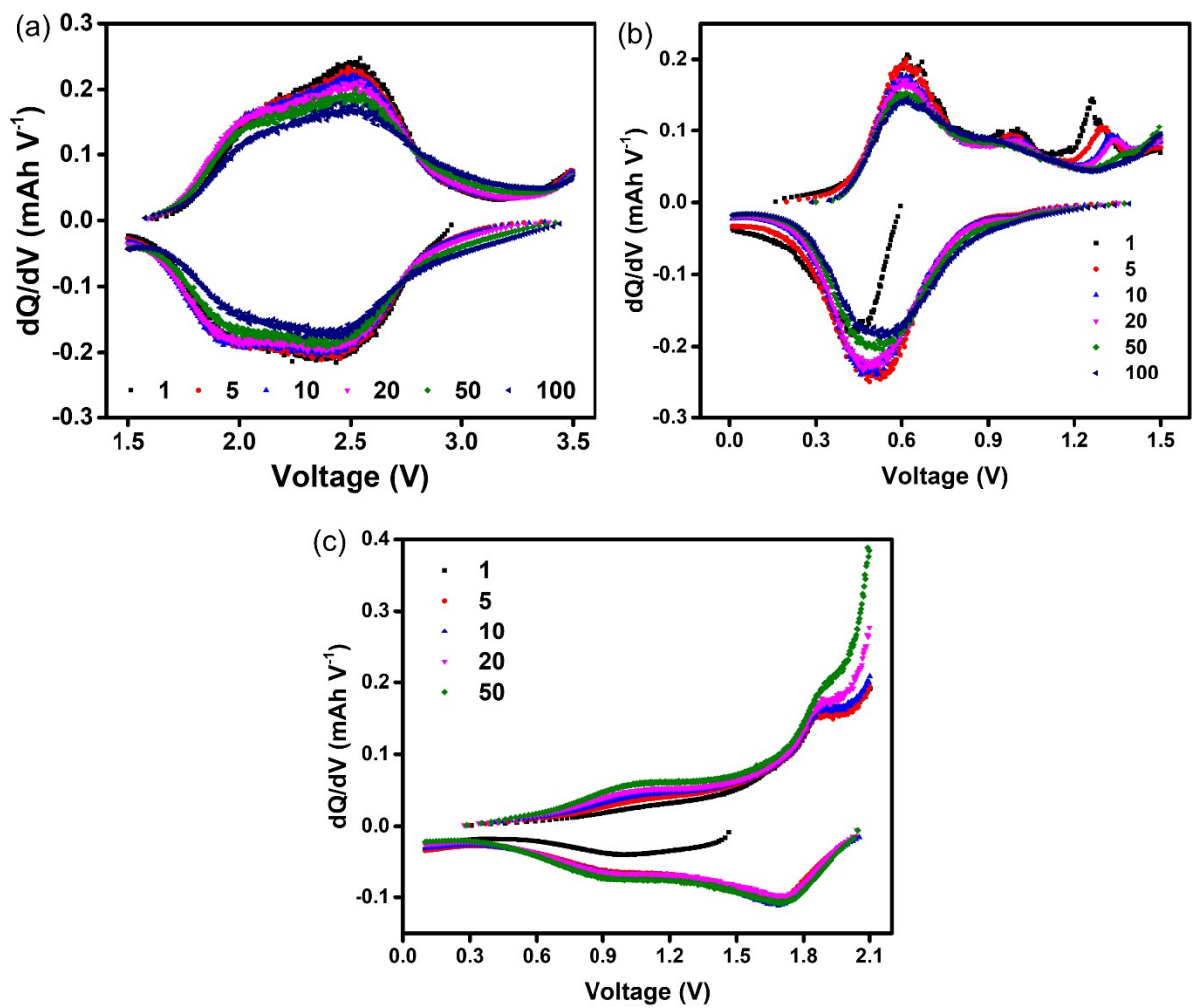
**Fig. S2.** X-ray diffraction pattern of the as prepared polymer.



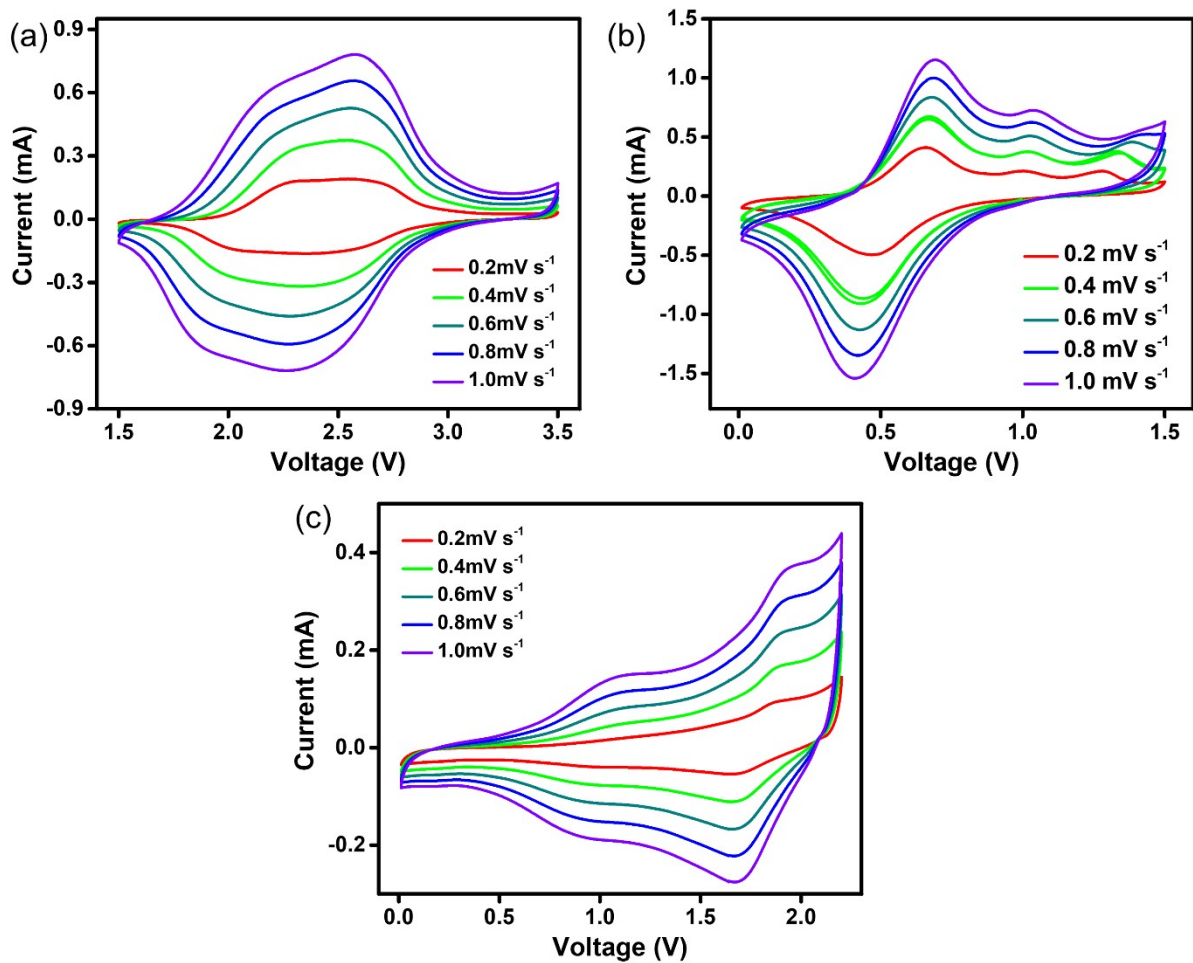
**Fig. S3.** Scanning electron microscopy image of the as prepared polymer.



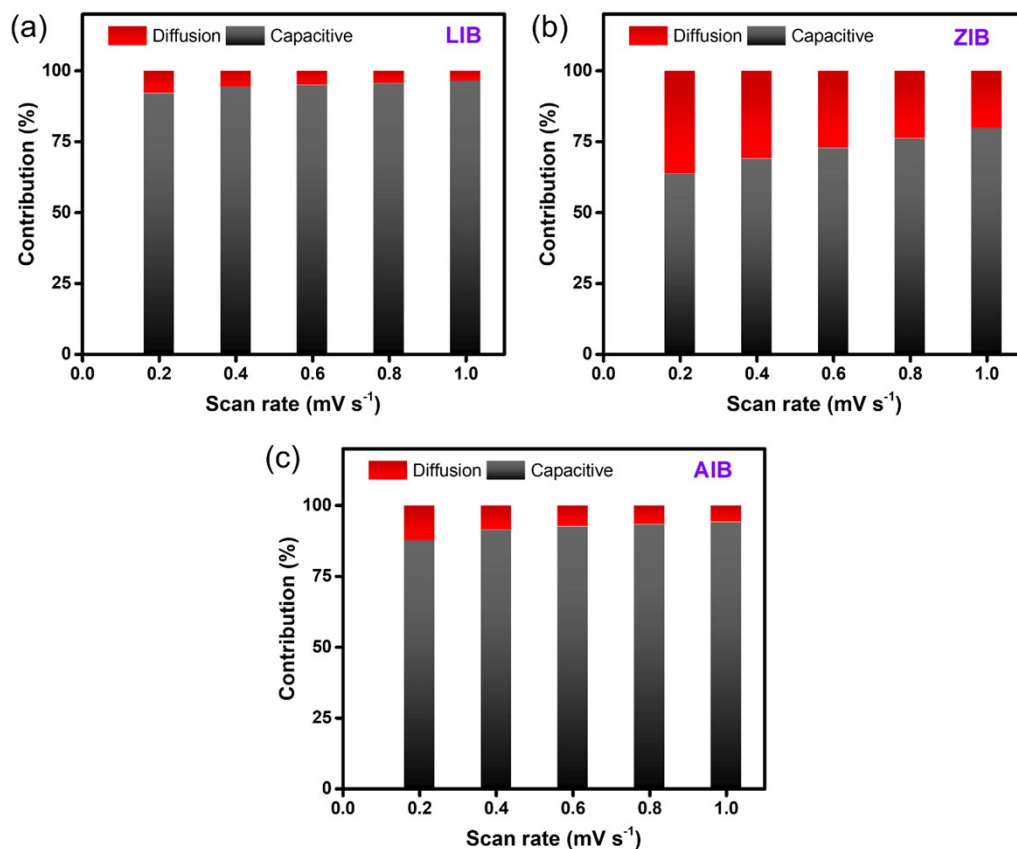
**Fig. S4.** Transmission electron microscopy image of the as prepared polymer.



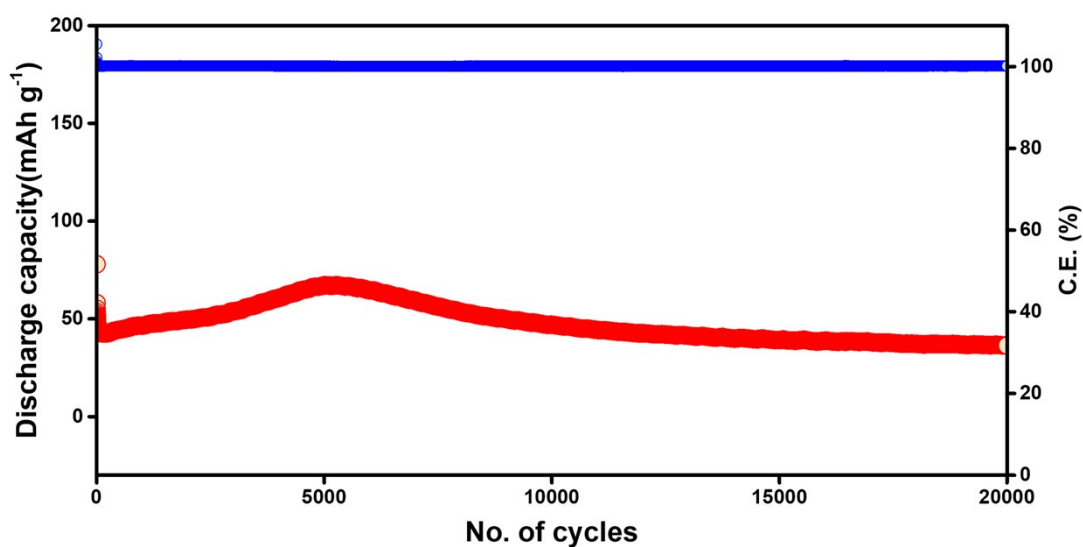
**Fig. S5.**  $dQ/dV$  plots obtained using 2DQP polymer electrodes at 100  $\text{mA g}^{-1}$  current density for (a) LIB, (b) ZIB and (c) AIB respectively.



**Fig. S6.** Cyclic voltammograms recorded at various scan rates from 0.2-1.0  $\text{mV s}^{-1}$  for (a) LIB, (b) ZIB and (c) AIB respectively.

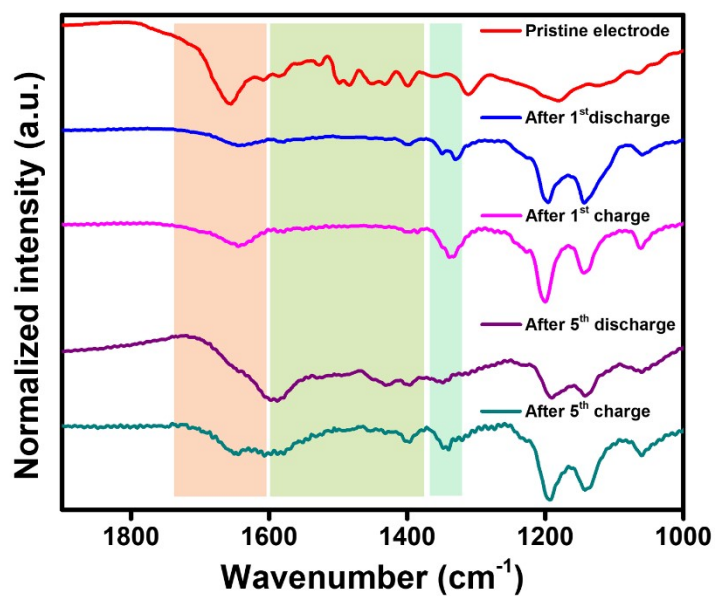


**Fig. S7.** Capacitive and diffusion contributions calculated at various scan rates from 0.2-1.0 mV s<sup>-1</sup> for (a) LIB, (b) ZIB and (c) AIB respectively.

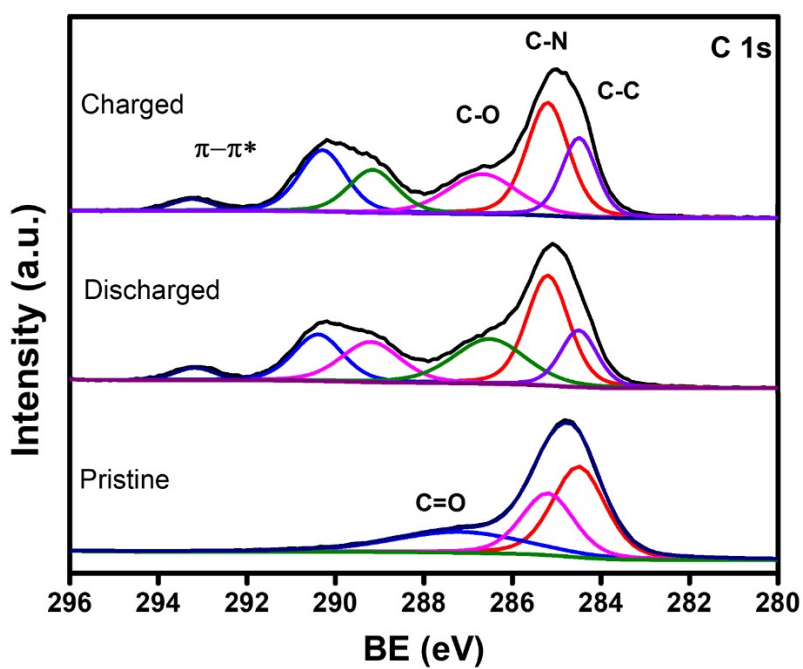


**Fig. S8.** Long term cycling of the polymer electrode at 2000 mA g<sup>-1</sup> current density for ZIB.

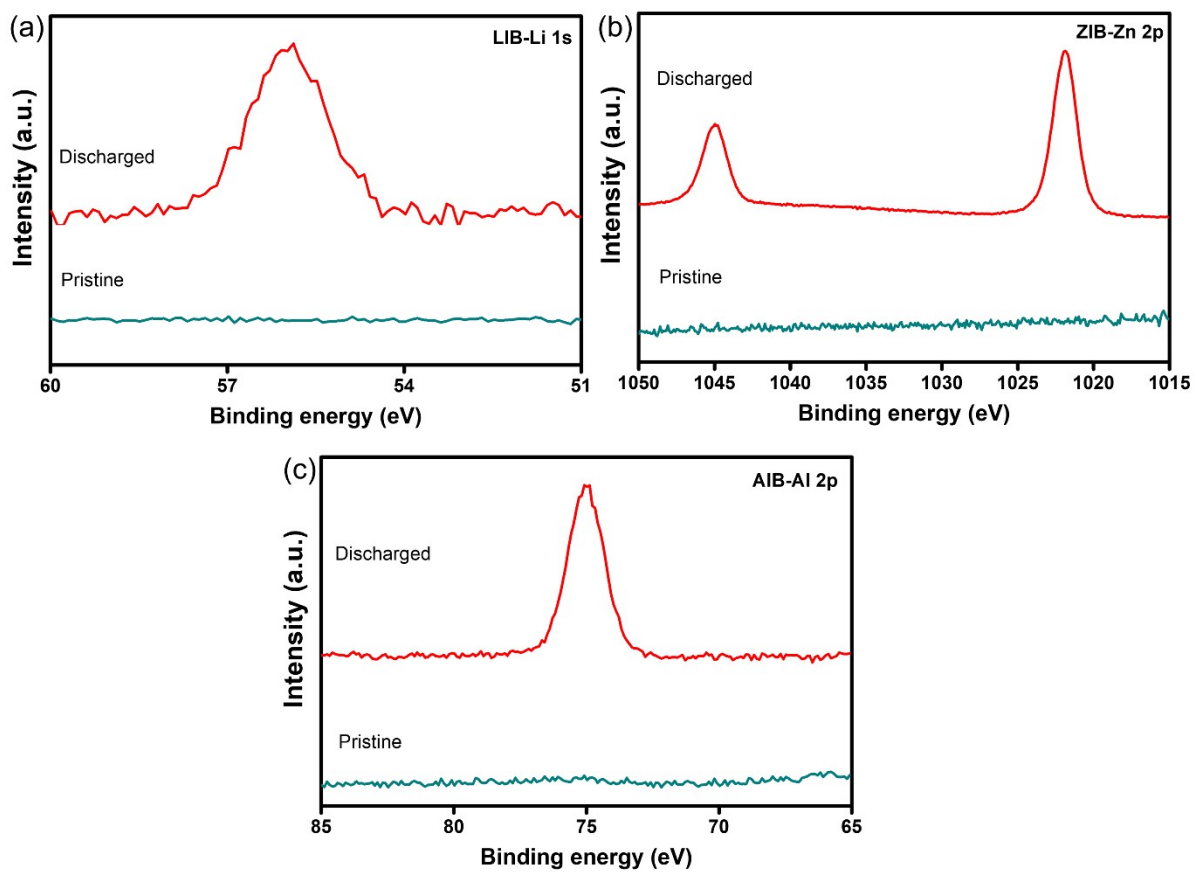




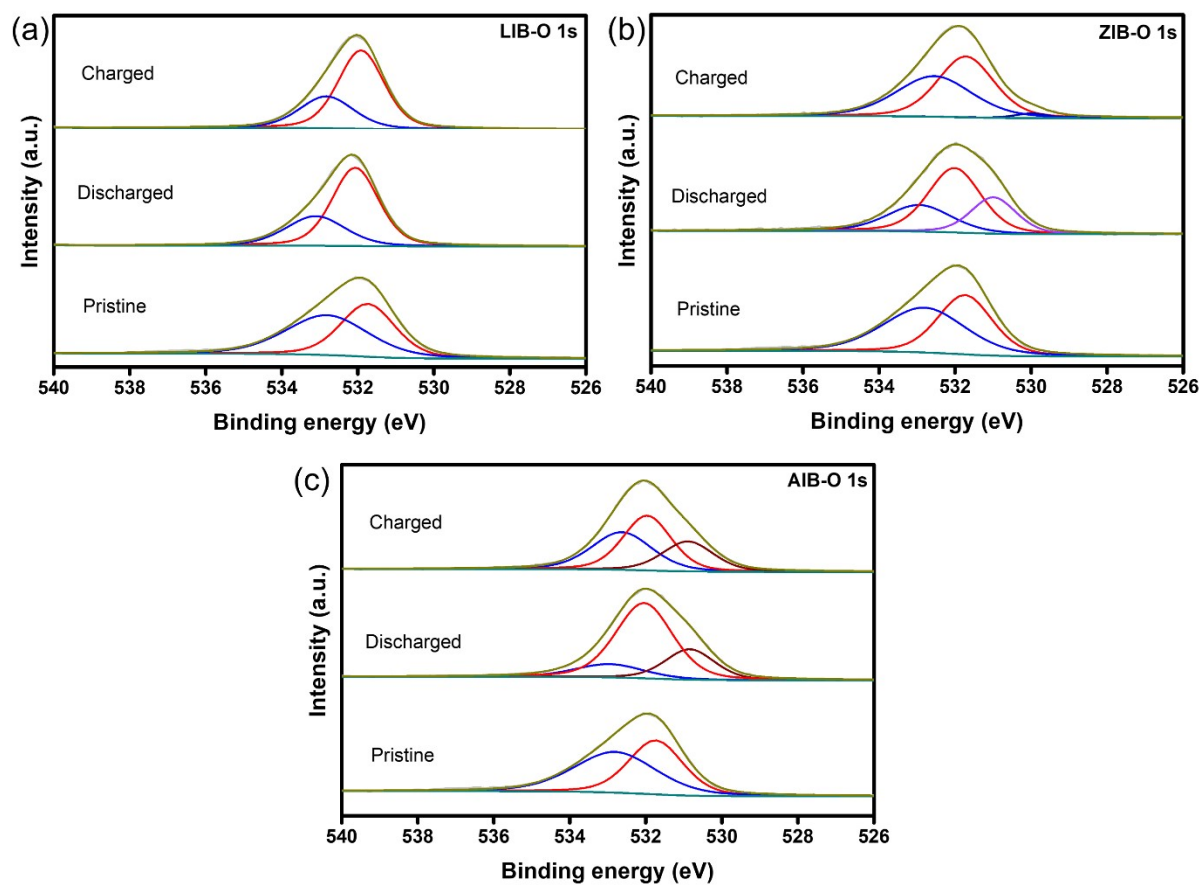
**Fig. S9.** Ex situ FT-IR spectra after different charge-discharge cycles of the polymer electrodes for LIBs.



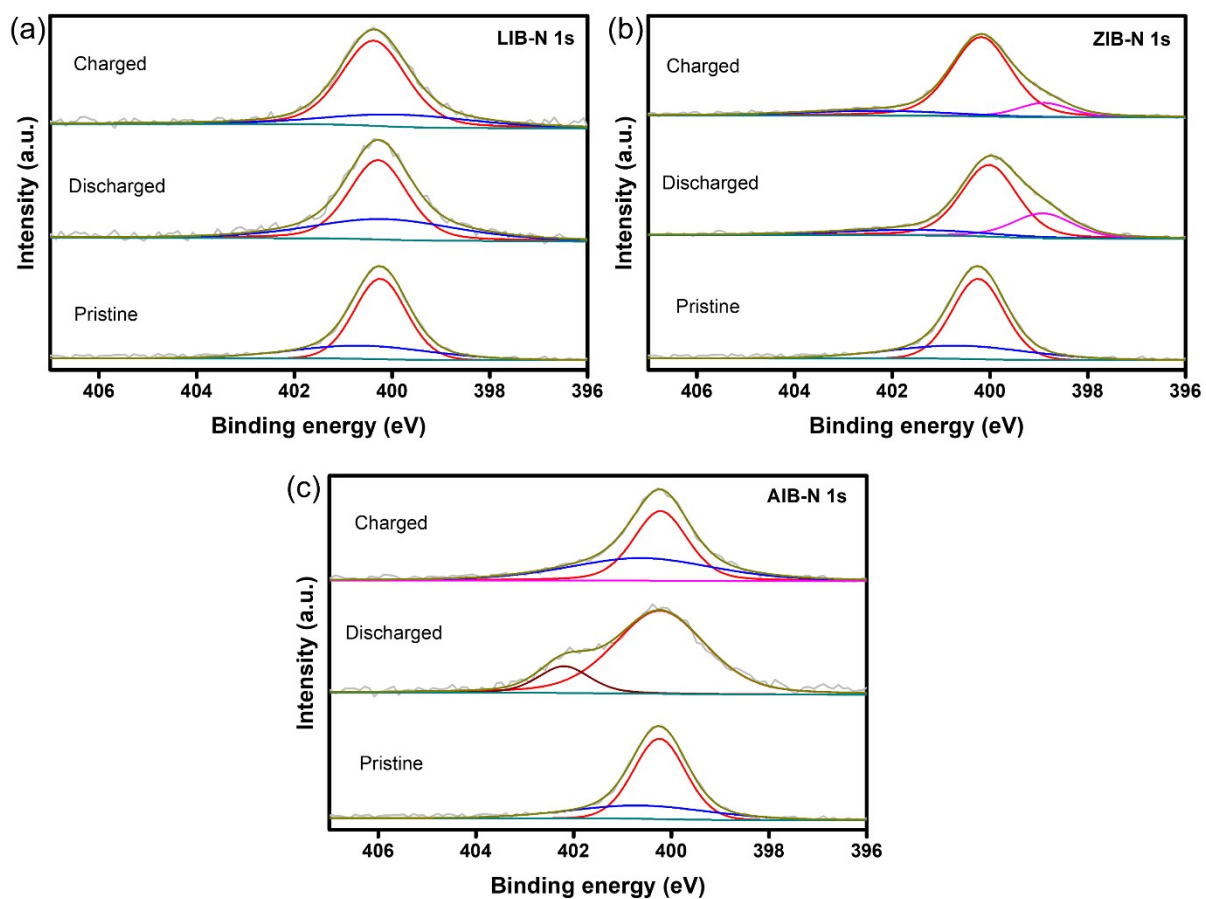
**Fig. S10.** High resolution XPS data for C 1s region after charge-discharge cycles for LIBs.



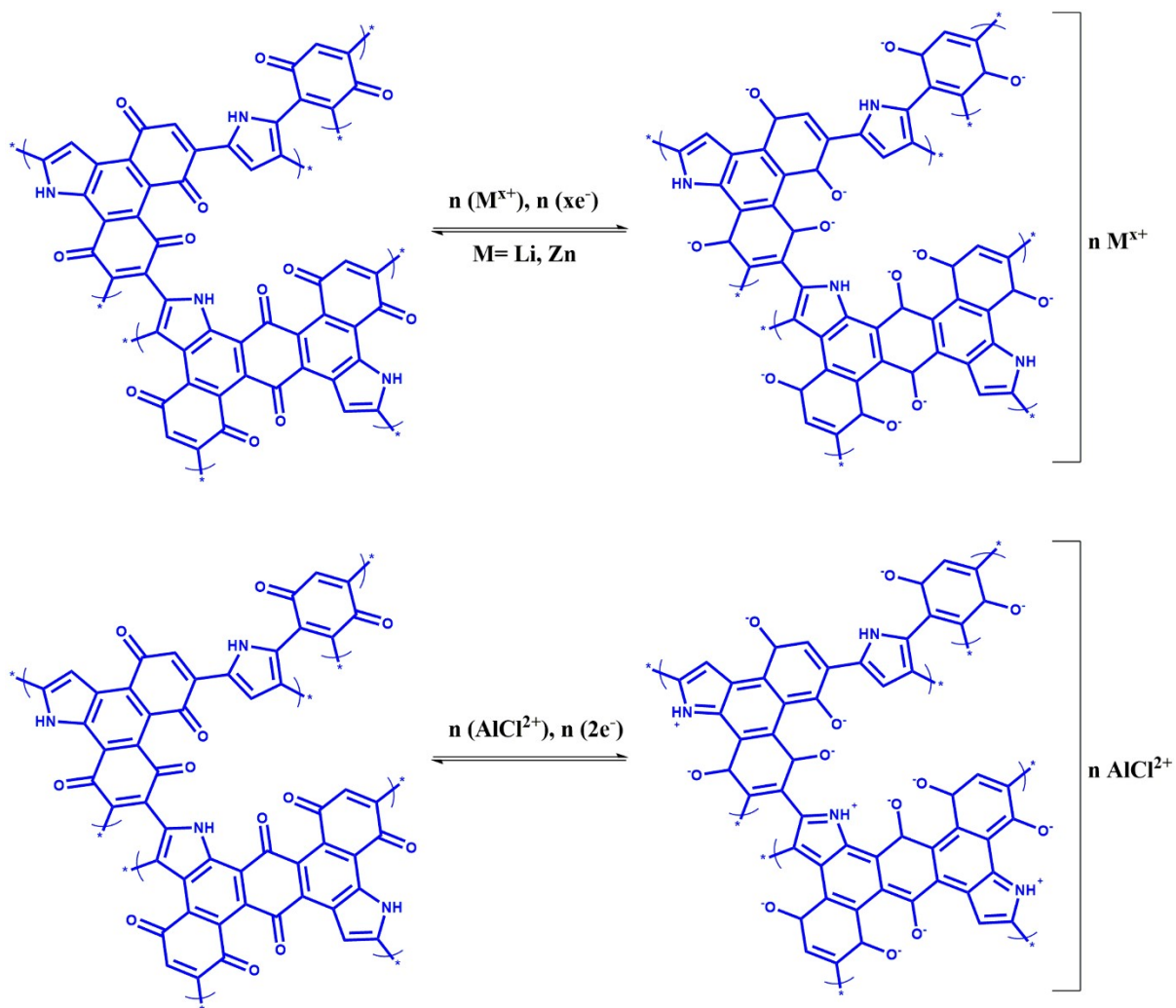
**Fig. S11.** High resolution XPS data for (a) Li 1s, (b) Zn 2p and (c) Al 2p regions after discharge for LIB, ZIB and AIB respectively.



**Fig. S12.** High resolution O 1s regions after charge-discharge cycles for (a) LIB, (b) ZIB and (c) AIB.

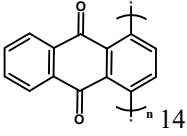
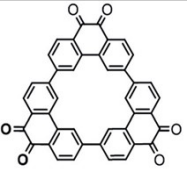


**Fig. S13.** High resolution N 1s regions after charge-discharge cycles for (a) LIB, (b) ZIB and (c) AIB.

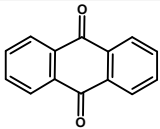
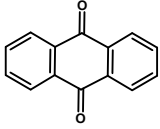


**Scheme S1.** Proposed ion storage mechanism for LIB, ZIB and AIB.

**Table S1.** Comparison of performance of reported quinone based ZIBs with the present study.

Electrode material	Electrolyte and potential window	Avg. voltage	Initial capacity at current density	Cycles	Rate performance	Ref.
DMBQ	0.5 M Zn(TFSI) <sub>2</sub> /AN 0-1.2 V	0.8 V	302.6 mAh g <sup>-1</sup> at 0.2 C	100	25 mAh g <sup>-1</sup> at 0.2 C	15
 PAQ	0.5 M Zn(TFSI) <sub>2</sub> /AN 0-1.2 V	0.5 V	42 mAh g <sup>-1</sup> at 0.2 C	100	15 mAh g <sup>-1</sup> at 0.2 C	15
PAQS	0.5 M Zn(TFSI) <sub>2</sub> /AN 0-1.2 V	0.5 V	70 mAh g <sup>-1</sup> at 0.2 C	-	25-30 mAh g <sup>-1</sup> at 0.2 C	15
 PQ-MCT	0.5 M Zinc triflate/DMF 0.1-1.7 V	0.75 V	145 mAh g <sup>-1</sup> at 50 mA g <sup>-1</sup>	20000	100 mAh g <sup>-1</sup> at 1000 mA g <sup>-1</sup>	16
Benzoquinone-pyrrole polymer	0.5 M Zn(TFSI) <sub>2</sub> /AN 0.01-1.5 V	~0.7V	65 mAh g <sup>-1</sup> at 100 mA g <sup>-1</sup>	10000	55 mAh g <sup>-1</sup> at 1000 mA g <sup>-1</sup>	This work

**Table S2.** Comparison of performance of quinone based electrodes for AIBs with the present study.

Electrode material	Electrolyte and potential window	Avg. voltage	Initial capacity at current density	Cycles	Rate performance and stability	Ref.
	EMImCl:AlCl <sub>3</sub> (1:1.5) 0.1-2.1 V	1.1 V	215.2 mAh g <sup>-1</sup> at 100 mA g <sup>-1</sup>	200	192.4 mAh g <sup>-1</sup> at 100 mA g <sup>-1</sup>	18
	EMImCl:AlCl <sub>3</sub> (1:1.5) 0.3-1.6 V	1.1 V	100 mAh g <sup>-1</sup> at 0.5 C	50	100 mAh g <sup>-1</sup> at 0.5 C	19
DMBQ	EMImCl:AlCl <sub>3</sub> (1:1.5) 0.3-1.6 V	1.5 V	210 mAh g <sup>-1</sup> at 40 mA g <sup>-1</sup>	-	-	19
PAQS/MWCNT	EMImCl:AlCl <sub>3</sub> (1:1.5) 0.4-1.8 V	1.0 V	190 mAh g <sup>-1</sup> at 0.5 C	500	114 mAh g <sup>-1</sup> at 0.5 C (60%)	19
Phenanthroquinone (PQ)	EMImCl:AlCl <sub>3</sub> (1:1.5) 0.8-1.8 V	1.35 V	176 mAh g <sup>-1</sup> at 0.5 C	50	-	20
Polyphenanthroquinone (pPQ)	EMImCl:AlCl <sub>3</sub> (1:1.5) 0.8-1.8 V	~1.4 V	24 mAh g <sup>-1</sup> at 0.5 C	500	30 mAh g <sup>-1</sup> at 10 C	20
PQ monomer	EMImAlCl <sub>4</sub> :AlCl <sub>3</sub> (1:1.3) 0.8-1.75 V	1.6 V	51 mAh g <sup>-1</sup> at 200 mA g <sup>-1</sup>	200	13 mAh g <sup>-1</sup> at 200 mA g <sup>-1</sup>	21
PQ trimer	EMImAlCl <sub>4</sub> :AlCl <sub>3</sub> (1:1.3) 0.8-1.75 V	1.6 V	27 mAh g <sup>-1</sup> at 200 mA g <sup>-1</sup>	200	17 mAh g <sup>-1</sup> at 200 mA g <sup>-1</sup>	21
PQ triangle	EMImAlCl <sub>4</sub> :AlCl <sub>3</sub> (1:1.3) 0.8-1.75 V	1.6 V	90 mAh g <sup>-1</sup> at 200 mA g <sup>-1</sup>	5000	53 mAh g <sup>-1</sup> at 200 mA g <sup>-1</sup>	21
Benzoquinone-pyrrole polymer	BMIImCl:AlCl <sub>3</sub> (1:1.5) 0.1-2.1 V	1.45 V	37.8 mAh g <sup>-1</sup> at 100 mA g <sup>-1</sup>	2000	82 mAh g <sup>-1</sup> at 1000 mA g <sup>-1</sup> (115%)	This work

**Table S3.** Atomic ratios (%) obtained from the *ex situ* XPS analysis of the electrodes in the case of AIBs.

Electrode	C 1s	N 1s	O 1s	F 1s	Cl 2p	Al 2p	Al/Cl
Pristine	77.01	5.88	17.11	-	-	-	-
Discharged	67.43	3.10	19.77	0.99	4.59	4.33	0.94

The *ex situ* XPS measurements were carried out at least at three different spots and the average values are given here.



## Quantification of peak areas for Figure 3c and 3d

Pristine electrode

Peak	C-C	C-N	C=O
Area (%)	44.3	30.7	25.96

For Zn-ion battery

Peak	C-C	C-N	C-O
Area of discharged electrode (%)	47.95	28.01	24.05
Area of charged electrode (%)	49.28	27.07	23.52

For Al-ion battery

Peak	C-C	C-N	C-O
Area of discharged electrode (%)	48.92	25.73	25.28
Area of charged electrode (%)	47.84	27.04	25.06

After charge-discharge experiments, along with C=O, C-N and C-O peaks, other peaks like C-F and  $\pi-\pi^*$  are observed. Hence, the areas for the peaks C=O, C-N and C-O are normalized to 100 %. The results suggest that all -C=O group are converted to enolate during discharge. After charging almost same area is observed but the peak positions are slightly shifted to higher binding energy values. This indicates that both C=O and C-O groups co-exist after charging.

### **Initial Coulombic efficiency**

The first cycle capacity is observed to be low since the potential range used is between the relatively low OCV values and the lower potential limit of cycling. In subsequent cycles, the potential range is large thereby contributing to high capacities and in turn high Coulombic efficiencies. The participation of the -N-H group in the Al-ion storage process is another possible reason for the observed low Coulombic efficiency in the initial stages.